

# Asymmetrization mechanism of jet profiles in decaying $\beta$ -plane turbulence

Keiichi Ishioka,\*

Division of Earth and Planetary Sciences, Graduate School of Science,

Kyoto University, Japan

Jitsuko Hasegawa,

Japan Meteorological Agency, Japan

and Shigeo Yoden

Division of Earth and Planetary Sciences, Graduate School of Science,

Kyoto University, Japan

October 18, 2006

---

\*ishioka@gfd-dennou.org

In our previous paper, asymmetry was found in jet profiles between eastward and westward jets which appear spontaneously in two-dimensional  $\beta$ -plane decaying turbulence. That is, westward jets are narrower and more intense than eastward jets. In this paper, we examine dependence of the asymmetry on the order of hyper-viscosity. It is shown that the dependence is not as strong as expected in our previous paper. A revised theoretical scenario to explain the weak dependence is also given.

# 1. Introduction

Spontaneous zonal jet formation is a well-known significant feature in two-dimensional  $\beta$ -plane turbulence (Rhines 1975; Vallis and Maltrud 1993). The formation itself is considered due to the upward cascade of energy which favors a zonal structure because of the  $\beta$  term. Vallis and Maltrud (1993) found asymmetry between eastward and westward jet profiles which emerged from turbulent states in the forced-dissipative numerical experiments. That is, eastward jets are narrower and more intense than westward jets. This asymmetry, which is also observed in two-dimensional forced-dissipative turbulence on a rotating sphere (Nozawa and Yoden 1997; Huang and Robinson 1998), is thought to be related to turbulent mixing of potential vorticity. Whether such asymmetry exists or not in decaying experiments, however, had not been explored until our previous paper, Hasegawa et al. (2006) (hereafter, HIY2006). In HIY2006, we conducted a large number of numerical experiments and found that there is asymmetry in profiles of zonal jets appearing spontaneously from  $\beta$ -plane decaying turbulence. That is, westward jets are narrower and more intense than eastward jets. This asymmetry, which is the reverse of that of the forced-dissipative cases, is also found by Lee and Smith (2006) in an early stage of the forced-dissipative case. In HIY2006, we also gave a theory to explain the asymmetry. Following the theory, it is expected that the significance of the asymmetry may strongly depend on the order of hyper-viscosity in the dissipation term. The dependence, however, was not explored in HIY2006. Therefore, in this paper, we examine the dependence of the significance.

The structure of this paper is as follows. The governing equation and experimental setup are given in Section 2. Results of numerical experiments are given and the dependence of the asymmetry of jet profiles on the order of hyper-viscosity is examined in Section 3. In Section 4, HIY2006's theory is revisited and a revised theory is given to explain a discrepancy between an expectation

from HIY2006's theory and the results of the present paper. Discussion and conclusions are given in Section 5.

## 2. Governing equation and experimental setup

The system under consideration is a non-divergent two-dimensional flow with hyper-viscosity on a  $\beta$ -plane. The flow is governed by the vorticity equation

$$\frac{\partial \zeta}{\partial t} + \frac{\partial \psi}{\partial x} \frac{\partial \zeta}{\partial y} - \frac{\partial \psi}{\partial y} \frac{\partial \zeta}{\partial x} + \beta \frac{\partial \psi}{\partial x} = (-1)^{p+1} \nu_p (\nabla^2)^p \zeta. \quad (1)$$

Here,  $\zeta \equiv \nabla^2 \psi$  is the vorticity,  $\psi$  is the stream-function,  $x$  is the longitude,  $y$  is the latitude,  $t$  is the time,  $\nabla^2$  is the Laplacian operator,  $\nu_p$  is the hyper-viscosity coefficient, and  $p$  is the order of the hyper-viscosity. Note that the governing equation has been nondimensionalized and we are dealing with nondimensional variables and parameters. We use three values of  $p$ ,  $p = 1, 2$ , and 3 to examine the dependence of the asymmetry of jet profiles on the order of the hyper-viscosity. Note that  $p = 1$  corresponds to Newtonian viscosity. The hyper-viscosity coefficient is set as small as possible unless enstrophy accumulates near the truncation wavenumber unphysically with the following experimental setup. Depending on  $p$ , we set the hyper-viscosity coefficient as follows:  $\nu_1 = 1 \times 10^{-4}$ ,  $\nu_2 = 1 \times 10^{-7}$ , and  $\nu_3 = 1 \times 10^{-11}$ .

We assume a periodic boundary condition in both  $x$  and  $y$  directions

$$\zeta(x, y + 2\pi, t) = \zeta(x, y, t) = \zeta(x + 2\pi, y, t). \quad (2)$$

To integrate Eq.(1) numerically, we adopted the Fourier spectral method with the truncation

wavenumber of  $K_T = 170$  for the spatial discretization. The nonlinear term is computed using the transform method with alias free grids,  $512 \times 512$ . The time integration scheme is the classical 4th order Runge-Kutta scheme.

The initial condition is a random vorticity field the energy spectrum  $E(K)$  of which is given as follows

$$E(K) \propto \left( \frac{2}{\sqrt{K/K_0} + \sqrt{K_0/K}} \right)^\gamma, \quad (3)$$

where,  $K = \sqrt{k^2 + l^2}$  is the total wavenumber,  $k$  is the wavenumber in the  $x$ -direction, and  $l$  is that in the  $y$ -direction. We set  $K_0 = 32$  and  $\gamma = 1000$ , which means the initial energy spectrum has a sharp peak at the wavenumber  $K = 32$ . The phase of each Fourier component is set randomly. We conduct 11-member ensemble experiments changing the random initial phase. The total energy of the initial state is set to  $1/2$ . This means that the root mean square velocity ( $u_0$ ) for the initial state is 1. We fix the parameter  $\beta$  as 256. This means that the Rhines wavenumber  $K_\beta = \sqrt{\beta/(2u_0)} = 8\sqrt{2} \approx 11.3$ . We checked that there is no qualitative difference in the following discussion with other sets of  $K_T$ ,  $K_0$ , and  $\beta$  as long as the inequality  $K_\beta \ll K_0 \ll K_T$  holds.

[Figure 1 about here.]

### 3. Results

Figure 1 shows the time evolution of the zonal mean zonal wind  $\bar{u}(y, t)$  for a member of ensemble experiments with  $p = 2$  (that is, the hyper-viscosity is of second power of Laplacian, which is also used in HIY2006). Here,  $u = -\partial\psi/\partial y$ , and  $(\bar{\cdot}) = \frac{1}{2\pi} \int_0^{2\pi} (\cdot) dx$ . As time goes on, zonal jet structures develop and the wavenumber of the zonal profile is close to  $K_\beta$  (in this particular example,

it is about 12). In an early stage of the time evolution ( $t \leq 2.0$ ), there is no significant difference between eastward and westward jets. After that, however, westward jets become more intense than eastward jets as found by HIY2006. Here, we define the intensity of a jet as the absolute value of the peak wind velocity. To confirm this asymmetry, we examine the time evolution of  $\bar{u}(y, t)$  of each ensemble member. We introduce a suffix  $j$  ( $j = 1, 2, \dots, 11$ ) to identify an ensemble member. Using this, we define the maximum speed of eastward and westward jets as

$$U_{\max}^e(t) = \max_{j \in \Lambda} (\max_{0 \leq y \leq 2\pi} u_j(y, t)), \quad (4)$$

$$U_{\max}^w(t) = \max_{j \in \Lambda} (\max_{0 \leq y \leq 2\pi} (-u_j(y, t))), \quad (5)$$

respectively. Here,  $\Lambda = \{1, 2, \dots, 11\}$ . Figure 2 shows the time evolutions of  $U_{\max}^e$  and  $U_{\max}^w$  for experiments with the hyper-viscosity of  $p = 2$ . Although there is no significant difference between  $U_{\max}^e$  and  $U_{\max}^w$  at an early stage of evolution ( $t \leq 1$ ),  $U_{\max}^w$  grows more rapidly than  $U_{\max}^e$  to have a larger value after that.

[Figure 2 about here.]

Until now, we have confirmed the asymmetry found by HIY2006 with ensemble experiments for  $p = 2$  hyper-viscosity. Following HIY2006's theory, which is reviewed in the next section, it is expected that the significance of the asymmetry may strongly depend on the order of hyper-viscosity  $p$ . Now, we examine the dependence of the significance. Figure 3 shows the time evolutions of  $U_{\max}^e$  and  $U_{\max}^w$  for  $p = 1$  (Newtonian viscosity) and  $p = 3$  (hyper-viscosity of the third power of Laplacian). There are some differences among Fig.2, Fig.3a, and Fig.3b in the timing when  $U_{\max}^w - U_{\max}^e$  starts growing and the value of  $U_{\max}^w - U_{\max}^e$  at later stages of the time evolutions. However, the dependence of the significance of the asymmetry on  $p$  is not as strong as

expected by HIY2006. In the next section, we review HIY2006's theory and propose a revised theory to explain the weak dependence.

[Figure 3 about here.]

## 4. Theory

In HIY2006, we proposed the following theoretical scenario to explain the asymmetry formation.

1. At the early stage of time evolution, weak zonal jets are formed by the upward energy cascade which favors zonal components in  $\beta$ -plane turbulence.
2. Considering Rossby wave propagation theory,  $l^2$  ( $l$  is the latitudinal wavenumber) of Rossby waves becomes so large in westward jet regions that Rossby waves are dissipated more easily than in eastward jet regions due to the hyper-viscosity.
3. When Rossby waves are dissipated, they leave their westward pseudo-momentum to zonal jets. Therefore, westward jets are intensified sharply.

To check the validity of the scenario, HIY2006 used a linearized equation of Eq.(1)

$$\frac{\partial \zeta'}{\partial t} + U_0(y) \frac{\partial \zeta'}{\partial x} + \left( \beta - \frac{\partial^2 U_0}{\partial y^2} \right) \frac{\partial \psi'}{\partial x} = (-1)^{p+1} \nu_p (\nabla^2)^p \zeta'. \quad (6)$$

Here,  $U_0(y)$  is a prescribed basic zonal flow, and  $\zeta' = \nabla^2 \psi'$ . The acceleration is evaluated as

$$\Delta U(y, t) = - \int_0^t \frac{\partial}{\partial y} (\overline{u'v'}) dt, \quad (7)$$

where  $u' = -\partial\psi'/\partial y$ ,  $v' = \partial\psi'/\partial x$ . To validate the scenario simply, we consider an idealized situation. The prescribed basic zonal flow profile is set as

$$U_0(y) = -A \sin(my). \quad (8)$$

The initial disturbance is set to be a monochromatic wave

$$\zeta'(x, y, t = 0) = B \sin(kx + ly), \quad (9)$$

where we set  $k = l = m = K_\beta$ ,  $A = 0.3$ , and  $B = 2K_\beta$ . The choice is based on representative values of the wavenumbers for both zonal components and wavy disturbances, and the speed of zonal jets in the nonlinear time evolution at  $t = 1$  when zonal jets start growing but the asymmetry has not yet developed. The value of  $B$  is set so that the energy of the monochromatic wave is  $1/2$ , which is the initial total energy of the nonlinear time evolution shown in the previous section. To integrate Eqs.(6) and (7) economically, we introduce a scale translation,

$$\begin{aligned} x_* &= K_\beta x, \quad y_* = K_\beta y, \quad \nabla_*^2 = K_\beta^{-2} \nabla^2, \quad \psi'_* = K_\beta^2 \psi', \quad U_{0*} = K_\beta U_0, \quad \Delta U_* = K_\beta \Delta U, \\ \beta_* &= K_\beta^{-1} \beta, \quad \nu_{p*} = K_\beta^{2p} \nu_p. \end{aligned}$$

Using this translation, Eqs.(6) and (9) are translated as follows

$$\frac{\partial \zeta'}{\partial t} + U_{0*} \frac{\partial \zeta'}{\partial x_*} + \left( \beta_* - \frac{\partial^2 U_{0*}}{\partial y_*^2} \right) \frac{\partial \psi'_*}{\partial x_*} = (-1)^{p+1} \nu_{p*} (\nabla_*^2)^p \zeta', \quad (10)$$

$$\zeta'(x_*, y_*, t = 0) = B \sin(x_* + y_*). \quad (11)$$

Integrating Eq.(10) from the initial condition Eq.(11) is easier than the original problem because we can reduce the truncation wavenumber for Fourier expansion. Time evolution of  $\Delta U(y, t)$  is computed as follows. Conceptually, spectrally discretized version of Eq.(10) can be written as

$$\frac{d\mathbf{x}}{dt} = \mathbf{M}\mathbf{x}. \quad (12)$$

Here,  $\mathbf{x}$  represents the vector of spectral coefficients of  $\psi'$ , and  $\mathbf{M}$  is a square matrix corresponding to the linear operators in Eq.(10). Equation(12) can be integrated analytically with the aid of numerical matrix diagonalization. The solution can be written as

$$\mathbf{x}(t) = \sum_n c_n e^{\sigma_n t} \mathbf{v}_n. \quad (13)$$

Here,  $\sigma_n$  and  $\mathbf{v}_n$  are an eigenvalue and a corresponding eigenvector of  $\mathbf{M}$ , respectively. The coefficient  $c_n$  is determined by the initial condition. In Eq.(7),  $\overline{\partial u'v'}/\partial y$  is a quadratic quantity of  $\psi'$ , so that the time integration can be done analytically using the solution, Eq.(13), for any  $t$  even for the limit  $t \rightarrow \infty$ . Figure 4 shows  $U(y, t) = U_0(y) + \Delta U(y, t)$  profile at  $t = 10$  and as  $t \rightarrow \infty$  for the hyper-viscosity of  $p = 2$ . As is expected in the scenario, the westward acceleration is sharper and more intense in the westward jet region than the eastward acceleration in the eastward jet region in Fig.4b (as  $t \rightarrow \infty$ ). However, the growth of the acceleration is very slow. At  $t = 10$  (Fig.4a), there can be seen the asymmetry, but the acceleration is not so significant as seen in Fig.2. Figure 5 shows  $U(y, t) = U_0(y) + \Delta U(y, t)$  profile as  $t \rightarrow \infty$  for  $p = 1$  (Newtonian viscosity) and  $p = 3$  hyper-viscosity. The asymmetry in final ( $t \rightarrow \infty$ ) acceleration is much more significant for  $p = 3$  hyper-viscosity than for  $p = 2$ , and it is much less significant for  $p = 1$  Newtonian viscosity.

The final acceleration profile depends mainly on the order of the hyper-viscosity when the hyper-viscosity coefficient is small enough. Figure 6 shows  $U(y, t)$  profile as  $t \rightarrow \infty$  for  $p = 1$  (Newtonian viscosity),  $p = 2$ , and  $p = 3$  hyper-viscosity with halved value of hyper-viscosity coefficients, that is,  $\nu_1 = 0.5 \times 10^{-4}$ ,  $\nu_2 = 0.5 \times 10^{-7}$ , and  $\nu_3 = 0.5 \times 10^{-11}$ . Comparing Fig.6a with Fig.5a, Fig.6b with Fig.4b, and Fig.6c with Fig.5b, it is hard to see the dependence of the final acceleration profile on the value of the hyper-viscosity coefficient. From further computations, it seems that the final acceleration profile converges to a profile which depends only on the order of the hyper-viscosity as  $\nu_p \rightarrow 0$  although we have no theoretical proof. Knowing this behavior of the final acceleration profile, we focus on the dependence of the acceleration profile on the order of the hyper-viscosity in this paper.

[Figure 4 about here.]

[Figure 5 about here.]

[Figure 6 about here.]

As seen above, there are two defects in HIY2006's theory. That is, the growth of the acceleration is too slow and the dependence of the acceleration asymmetry on  $p$  is too strong comparing with the results of nonlinear time evolution seen in the previous section. Therefore, we now try to revise the scenario to fill the gap. In the scenario and the computation, we neglected two important effects. One is the effect that the acceleration changes the basic profile, which will affect Rossby wave propagation. The other is the effect of hyper-viscosity on the basic profile, which will smooth it. To include these effects, we change Eq.(6) into

$$\frac{\partial \zeta'}{\partial t} + U(y, t) \frac{\partial \zeta'}{\partial x} + \left( \beta - \frac{\partial^2 U}{\partial y^2} \right) \frac{\partial \psi'}{\partial x} = (-1)^{p+1} \nu_p (\nabla^2)^p \zeta', \quad (14)$$

and let  $U$  change as

$$\frac{\partial U(y, t)}{\partial t} = -\frac{\partial}{\partial y}(\overline{u'v'}) + (-1)^{p+1}\nu_p(\nabla^2)^p U. \quad (15)$$

We integrate Eqs.(14) and (15) simultaneously from the initial condition  $U(y, t = 0) = U_0(y)$  with the scale translation described above. These coupled equations form a nonlinear system, so that the time integration is done numerically using the classical 4th order Runge-Kutta scheme. Figure 7 shows  $U(y, t)$  profiles at  $t = 10$  computed for  $p = 1, 2,$  and  $3$ . In Fig.7, each figure shows sharp acceleration in the westward jet region and the intensity of the acceleration is large enough even at  $t = 10$ , but the difference of the acceleration among the figures is not so large as that between Fig.4 and Fig.5.

To check which of the two effect, the change in the basic profile and the hyper-viscosity on the zonal mean flow, is important, we conduct an additional set of computations removing the hyper-viscosity term in the time evolution equation of the zonal mean flow (Eq.(15)). Figure 8 shows resulting  $U(y, t)$  profiles at  $t = 10$  computed for  $p = 1, 2,$  and  $3$ . The difference of the acceleration among the figures in Fig.8 is as inconspicuous as that in Fig.7. Therefore, it is concluded that the effect of the hyper-viscosity on the zonal mean flow is much less important for reducing the dependence of the acceleration on the order of the hyper-viscosity.

Although the results above indicate that the wave-mean-flow interaction can explain the asymmetry in the acceleration profile and the insignificant dependence on the order of the hyper-viscosity, they are based on the quasi-linear system consists of Eqs.(14) and (15), which neglects the wave-wave interactions. To examine whether the wave-wave interactions can affect the acceleration profile largely or not, we conduct a further set of computations. The full nonlinear governing equation, Eq.(1), is integrated from the same initial condition as used in the quasi-linear system

above. That is, the initial  $\zeta$  field can be written as

$$\zeta(x, y, t = 0) = -\frac{dU_0}{dy} + \zeta'(x, y, t = 0) = Am \sin(my) + B \sin(kx + ly) \quad (16)$$

using Eqs.(8) and (9). Figure 9 shows resulting zonal mean flow profile  $\bar{u}(y, t)$  at  $t = 10$  computed for  $p = 1, 2,$  and  $3$ . Comparing Fig.9 with Fig.7, the acceleration profiles are very similar for each  $p$ . This result indicates that the wave-wave interactions are much less important for the asymmetric acceleration than the wave-mean-flow interactions. The reason the wave-wave interactions have secondary importance is thought that the wave-mean-flow interactions affect the characteristics of the wave propagation dominantly through the change in the mean flow profile while waves of higher wavenumbers generated by the wave-wave interactions are transient and have little effect on the propagation of the primary wave.

[Figure 7 about here.]

[Figure 8 about here.]

[Figure 9 about here.]

## 5. Discussion and Conclusions

One main conclusion of this paper is that the asymmetry found by HIY2006, which is that westward jets are more intense than eastward jets in  $\beta$ -plane decaying turbulence, can be seen even if we adopt Newtonian viscosity not hyper-viscosity. That is, the asymmetry is not an illusion arising from hyper-viscosity. This weak dependence of the asymmetry on the order of hyper-viscosity  $p$  is somewhat in discord with HIY2006's theory. This discordance is resolved with a revision for the

theory as seen in the previous section. The effect which is thought to prevent the dependence from becoming too strong is the acceleration by Rossby waves changes the basic profile, which causes a positive feedback to magnify the asymmetry. The reason the effect lead to the weak dependence on the order of the hyper-viscosity is explained as follows. Once westward acceleration occurs in westward jet region, the speed of westward jet is amplified so that it becomes closer to the phase speed of Rossby waves. Then  $l^2$  of Rossby waves becomes so large there (if a critical level appear,  $l^2$  goes to infinity) that the waves are dissipated very quickly independently of the order of the hyper-viscosity. Therefore, even in Newtonian viscosity case, the asymmetry can grow quickly. We should now add a new item to the scenario reviewed in the previous section as,

4. The acceleration causes a positive feedback to help the asymmetry to grow. By this effect, the significance of the asymmetry does not strongly depend on the order of hyper-viscosity.

Now, a question comes into mind naturally. Why does the mechanism fail to work in forced cases? We speculate that there are two reasons. One is that continuous energy input in small scales in forced cases keeps nonlinear terms dominant. This effect prevents the mechanism from working well because it is based on linear wave dynamics. Stronger zonal jets in forced cases make  $\hat{\beta} = \beta - \bar{u}_{yy}$  small in westward jet regions, which may promote the dominance of nonlinear terms further. The other is the Rayleigh friction type drag term introduced in forced cases to obtain energy equilibration. If such a damping term causes large scale wave dissipation dominantly, it will also prevent the mechanism from working well because scale dependence of dissipation is necessary for the mechanism to work. The importance of the drag term to obtain stronger eastward jets than westward jets is shown by Lee and Smith (2006). Further investigation, however, is required to confirm whether the speculation above is correct or not.

## **Acknowledgements**

The authors would like to thank two anonymous reviewers for their helpful and constructive comments on this work. Numerical library ISPACK (Ishioka 2005) is used for the computations. GFD-DENNOU Library (SGKS Group 1995) is used for drawing the figures.

## References

- Hasegawa, J., K. Ishioka, and S. Yoden, 2006: Asymmetrization of jet profiles in  $\beta$ -plane turbulence. *IUTAM Symposium on Elementary Vortices and Coherent Structures; Significance in Turbulence Dynamics*, S. Kida, Ed., Springer, 207 – 211.
- Huang, H.P., and A. Robinson, 1998: Two-dimensional turbulence and persistent zonal jets in a global barotropic model. *J. Atmos. Sci.*, **55**, 611 – 632.
- Ishioka, K., 2005: ISPACK-0.71, <http://www.gfd-dennou.org/arch/ispack/>, GFD-Dennou Club (in Japanese).
- Lee, Y., and L. M. Smith, 2006: A mechanism for the formation of geophysical and planetary zonal flows. *Preprint*.
- Nozawa, T., and S. Yoden, 1997: Formation of zonal band structure in forced two-dimensional turbulence on a rotating sphere. *Phys. Fluids*, **9**, 2081 – 2093.
- Rhines, P. B., 1975: Waves and turbulence on a beta-plane. *J. Fluid Mech.*, **69**, 417 – 443.
- SGKS Group, 1995: DCL-5.1, <http://www.gfd-dennou.org/library/dcl/>, GFD-Dennou Club (in Japanese).
- Vallis, G. K., and M. E. Maltrud, 1993: Generation of mean flows and jets on a beta plane and over topography. *J. Phys. Oceanogr.*, **23**, 1346 – 1362.

# List of Figures

1	Time evolution of the zonal mean zonal wind profile $\bar{u}(y, t)$ for a member of ensemble experiments with $p = 2$ hyper-viscosity. Time $t$ is indicated on the top of each figure. . . . .	17
2	Time evolutions of $U_{\max}^w$ (solid line) and $U_{\max}^e$ (dotted line) with $p = 2$ hyper-viscosity. . . . .	18
3	Same as Fig.2 but for $p = 1$ Newtonian viscosity (a) and $p = 3$ hyper-viscosity (b). . . . .	19
4	Acceleration by an initially monochromatic Rossby wave in the linearized model Eqs.(6) and (7) for $p = 2$ hyper-viscosity. The dotted line shows the prescribed zonal flow profile $U_0$ , and the solid line shows $U_0 + \Delta U$ profile. (a) is at $t = 10$ , and (b) is as $t \rightarrow \infty$ . . . . .	20
5	Same as Fig.4b but for $p = 1$ Newtonian viscosity (a), and for $p = 3$ hyper-viscosity (b). . . . .	21
6	Same as Fig.4b and Fig.5 except that the value of hyper-viscosity coefficient is halved. (a) is for $p = 1$ Newtonian viscosity, (b) is for $p = 2$ hyper-viscosity, and (c) is for $p = 3$ hyper-viscosity. . . . .	22
7	Acceleration by an initially monochromatic Rossby wave in the linearized model Eqs.(14) and (15) at $t = 10$ . The dotted line shows the prescribed zonal flow profile $U_0$ , and the solid line shows $U$ profile. (a) is for $p = 1$ Newtonian viscosity, (b) is for $p = 2$ hyper-viscosity, and (c) is for $p = 3$ hyper-viscosity. . . . .	23
8	Same as Fig.7 except that the acceleration is calculated without the hyper-viscosity term in Eq.(15). . . . .	24

9 Same as Fig.7 except that the acceleration is calculated with the full nonlinear  
equation, Eq.(1). . . . . 25

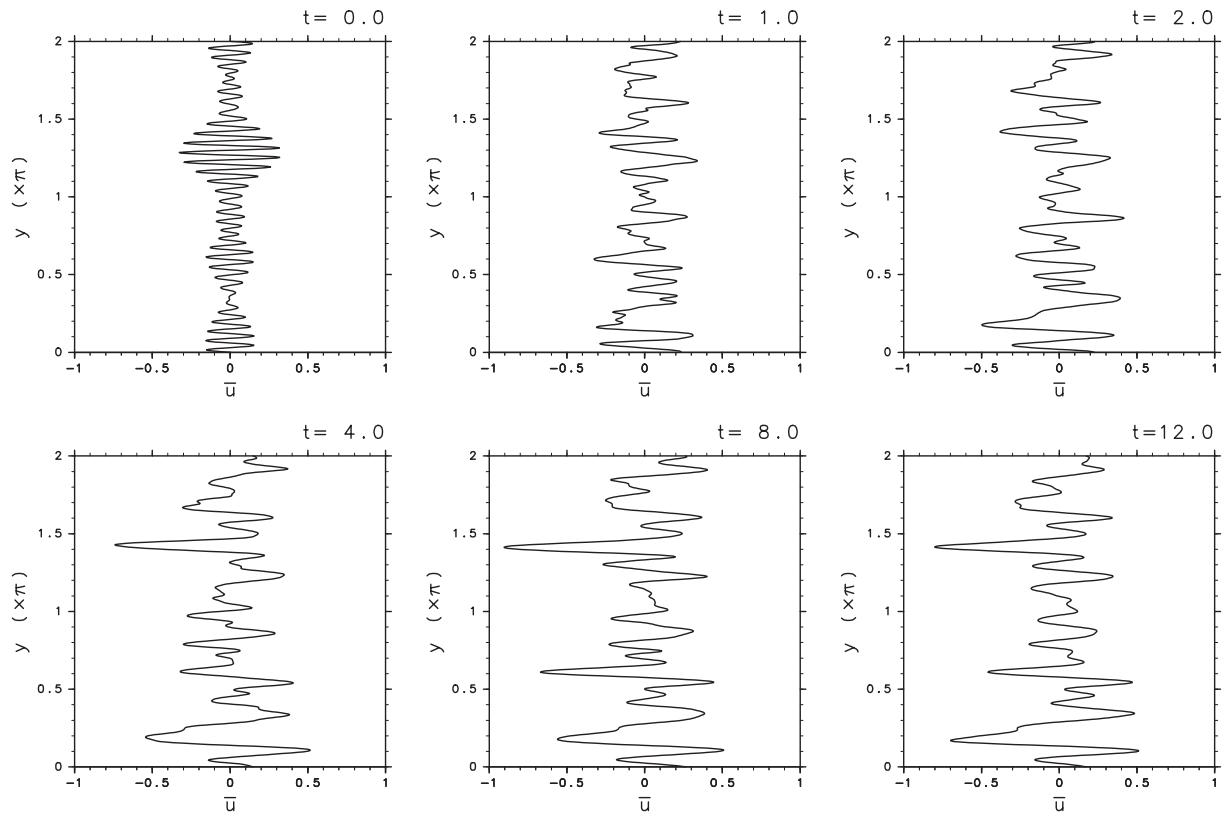


Figure 1: Time evolution of the zonal mean zonal wind profile  $\bar{u}(y, t)$  for a member of ensemble experiments with  $p = 2$  hyper-viscosity. Time  $t$  is indicated on the top of each figure.

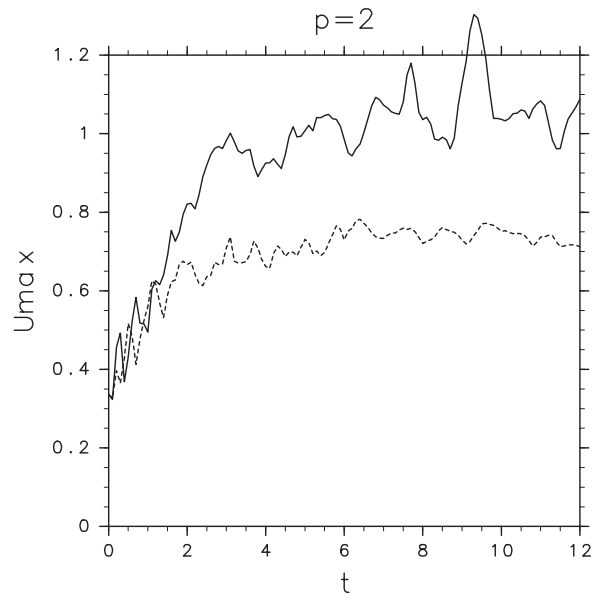


Figure 2: Time evolutions of  $U_{\max}^w$  (solid line) and  $U_{\max}^e$  (dotted line) with  $p = 2$  hyper-viscosity.

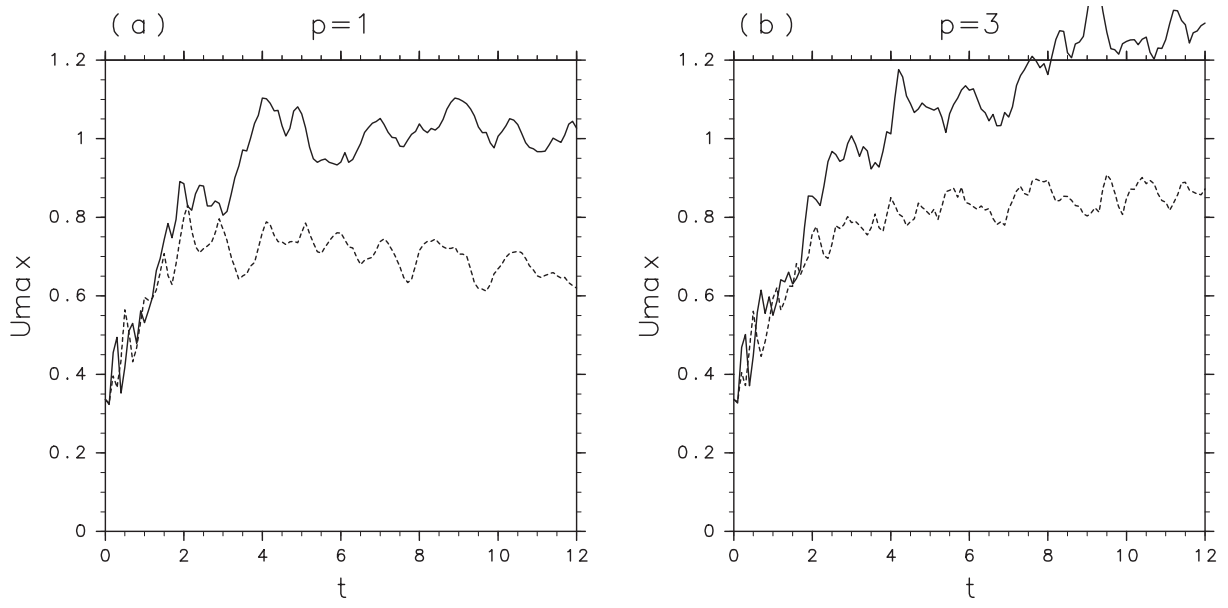


Figure 3: Same as Fig.2 but for  $p = 1$  Newtonian viscosity (a) and  $p = 3$  hyper-viscosity (b).

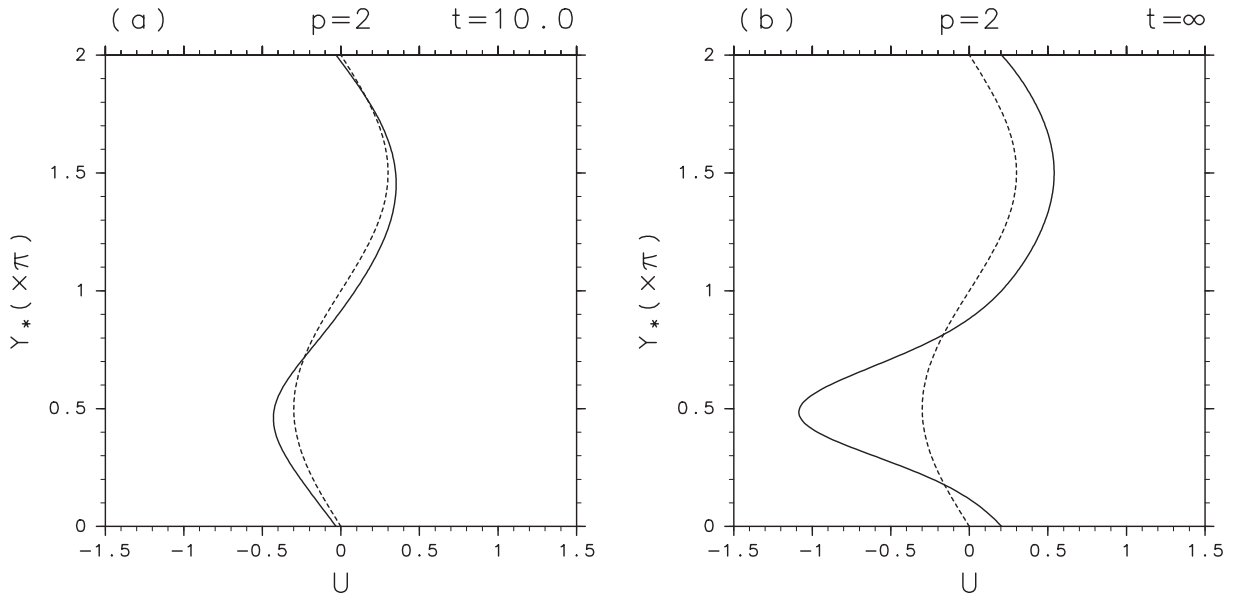


Figure 4: Acceleration by an initially monochromatic Rossby wave in the linearized model Eqs.(6) and (7) for  $p = 2$  hyper-viscosity. The dotted line shows the prescribed zonal flow profile  $U_0$ , and the solid line shows  $U_0 + \Delta U$  profile. (a) is at  $t = 10$ , and (b) is as  $t \rightarrow \infty$ .

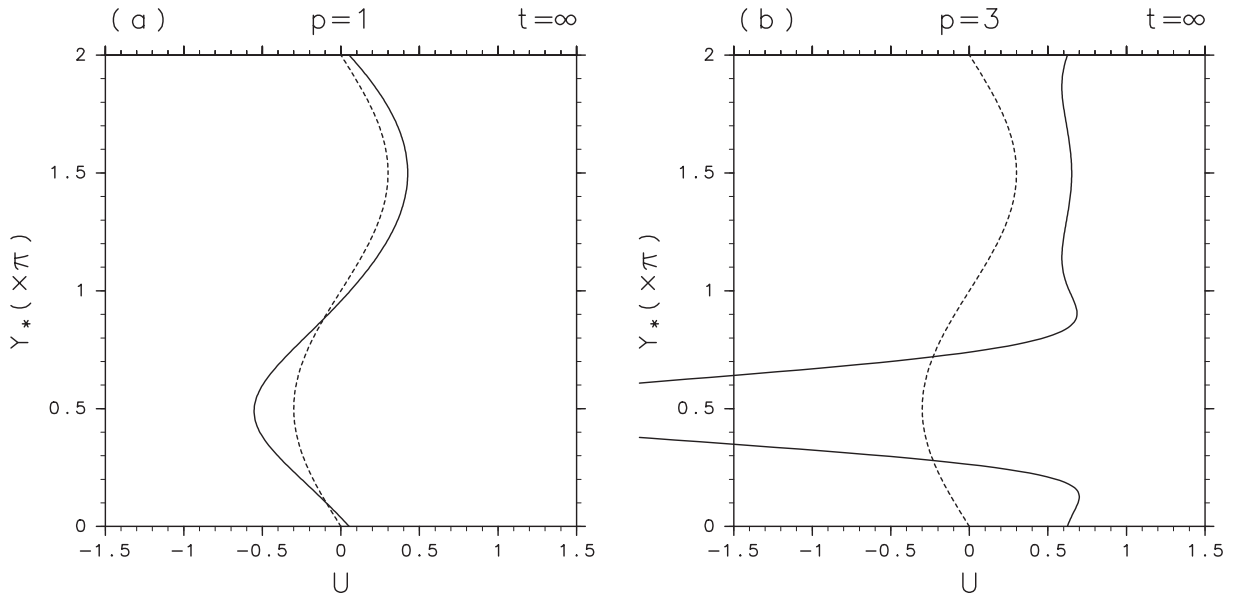


Figure 5: Same as Fig.4b but for  $p = 1$  Newtonian viscosity (a), and for  $p = 3$  hyper-viscosity (b).

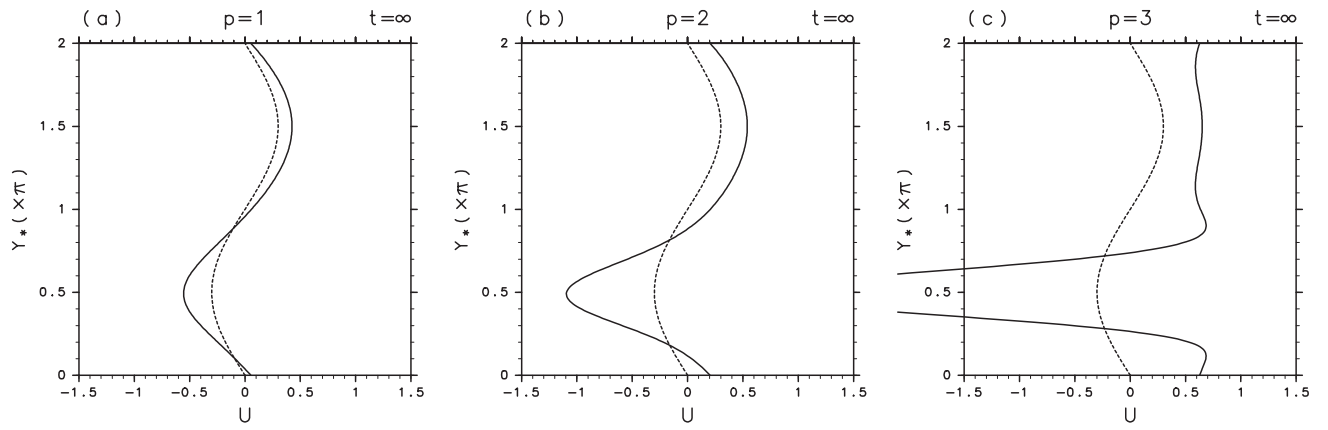


Figure 6: Same as Fig.4b and Fig.5 except that the value of hyper-viscosity coefficient is halved. (a) is for  $p = 1$  Newtonian viscosity, (b) is for  $p = 2$  hyper-viscosity, and (c) is for  $p = 3$  hyper-viscosity.

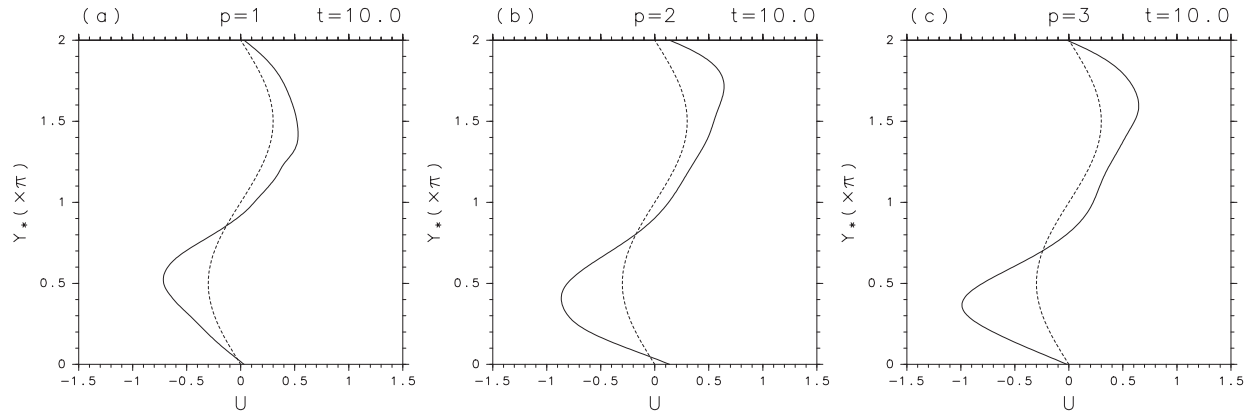


Figure 7: Acceleration by an initially monochromatic Rossby wave in the linearized model Eqs.(14) and (15) at  $t = 10$ . The dotted line shows the prescribed zonal flow profile  $U_0$ , and the solid line shows  $U$  profile. (a) is for  $p = 1$  Newtonian viscosity, (b) is for  $p = 2$  hyper-viscosity, and (c) is for  $p = 3$  hyper-viscosity.

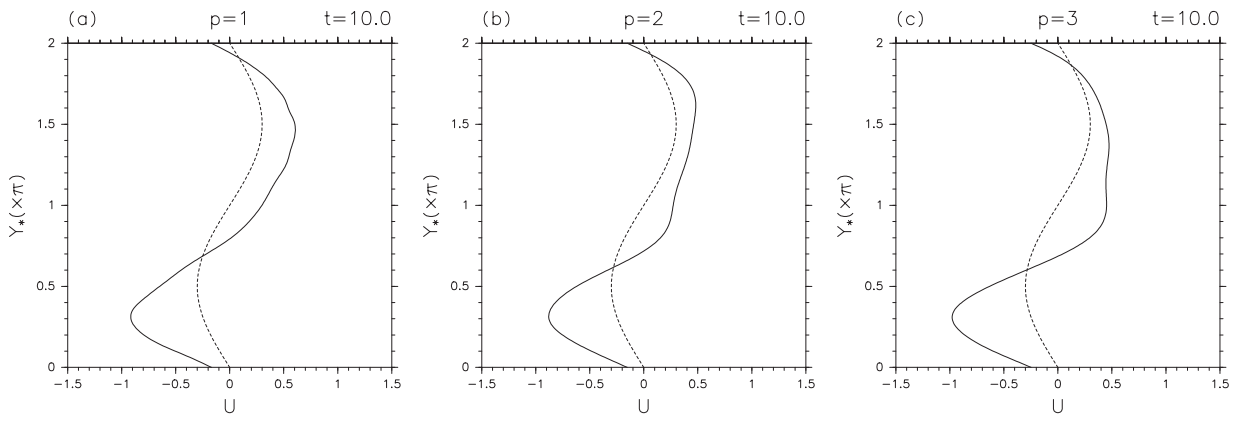


Figure 8: Same as Fig.7 except that the acceleration is calculated without the hyper-viscosity term in Eq.(15).

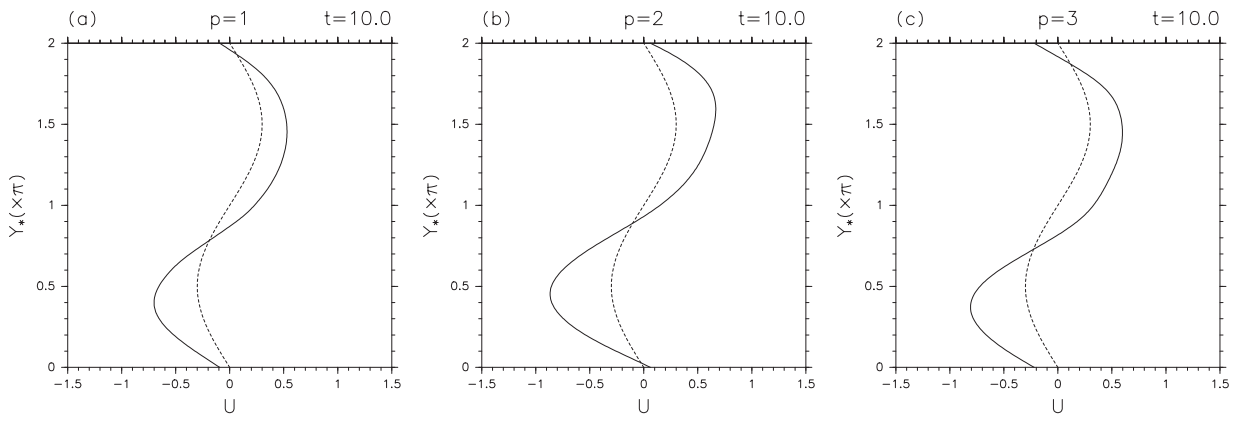


Figure 9: Same as Fig.7 except that the acceleration is calculated with the full nonlinear equation, Eq.(1).